NUCL SCI TECH (2016) 27:130
DOI 10.1007/s41365-016-0139-x

Chiral phase transition of quark matter in the background of parallel electric and magnetic fields

M. Ruggieri[1] · Guang-Xiong Peng[1,2]

Received: 15 August 2016 / Revised: 30 August 2016 / Accepted: 1 September 2016 / Published online: 11 October 2016

Abstract We report on our results about spontaneous chiral symmetry breaking for quark matter in the background of static and homogeneous parallel electric field, $\boldsymbol{E}$, and magnetic field, $\boldsymbol{B}$. A Nambu–Jona–Lasinio model is used to compute the dependence of the chiral condensate at finite temperature, E and B. We study the effect of this background on inverse catalysis of chiral symmetry breaking for E and B of the same order of magnitude. We also consider the effect of equilibration of chiral density, n_5, produced by axial anomaly on the critical temperature. The equilibration of n_5 allows for the introduction of the chiral chemical potential, μ_5, which is computed self-consistently as a function of temperature and field strength. We find that even if the chiral medium is produced by the fields the thermodynamics, with particular reference to the inverse catalysis induced by the external fields, it is not very affected by n_5 at least if the average μ_5, at equilibrium is not too large.

This work was supported by the CAS President's International Fellowship Initiative (No. 2015PM008), and the National Natural Science Foundation of China (Nos. 11135011 and 11575190).

✉ M. Ruggieri
marco.ruggieri@ucas.ac.cn

Guang-Xiong Peng
gxpeng@ucas.ac.cn

1 College of Physics, University of Chinese Academy of Sciences, Yuquanlu 19A, Beijing 100049, China

2 Theoretical Physics Center for Science Facilities, Institute of High Energy Physics, Beijing 100049, China

Keywords Chiral chemical potential · Nambu–Jona–Lasinio model · Chiral phase transition in parallel electric and magnetic fields

1 Introduction

Systems with a finite chiral density, $n_5 \equiv n_R - n_L$, have attracted some interest recently. A medium with chirality imbalance can be obtained dynamically because of quantum anomaly [1, 2] when fermions interact with nontrivial gauge field configurations. In the context of quantum chromodynamics (QCD), some of these configurations at finite temperature in Minkowski space are named sphalerons, being characterized by parallel chromo-electric and chromo-magnetic fields and whose production rate has been estimated to be quite large at large temperature [3, 4]. The large number of sphaleron transitions in high temperature suggests the possibility that net chirality might be locally abundant in the quark–gluon plasma phase of QCD, when one couples this thermal QCD bath with an external strong magnetic field, $\boldsymbol{B}$, produced in the early stages of heavy ion collisions, the coexistence of $n_5 \neq 0$ and $\boldsymbol{B} \neq 0$ might lead to the Chiral Magnetic Effect (CME) [5, 6]. Besides CME other interesting effects related to anomaly and chiral imbalance can be found in [7–21].

In order to describe systems with finite chirality in thermodynamical equilibrium, it is possible to introduce the conjugated chemical potential, named the chiral chemical potential, μ_5 [22–43]. The chiral chemical potential describes a system in which chiral density is in thermodynamical equilibrium; naming τ the time scale in which n_5 equilibrates, one might assume that $\mu_5 \neq 0$ describes a system in thermodynamical equilibrium with a fixed value of n_5 on a time scale much larger than τ.

In this talk, we report about chiral phase transition and chiral density production in the context of quark matter in a background static and homogeneous parallel electric, $\boldsymbol{E}$, and magnetic, $\boldsymbol{B}$, fields. This particular field configuration is interesting in the context of a medium with chirality imbalance because it produces dynamically a chiral density thanks to the anomaly. Firstly, we focus on the critical temperature for chiral symmetry restoration, T_c, in presence of the external fields. This part of the study completes previous studies about chiral symmetry breaking/restoration in the background of external fields [44–54]. We find that the effect of the electric field is to lower the critical temperature, and this inverse catalysis scenario does not change considerably when the magnetic field is added, as long as the magnetic field is not very large compared to the electric one.

We are also interested in studying the effect of chiral density on the thermodynamics of the system, following our previous studies [36, 37]. In our context, n_5 is produced thanks to the quantum anomaly by $\boldsymbol{E}\cdot\boldsymbol{B}\neq 0$ and equilibrates because of the existence of chirality changing processes in the thermal bath that relax on a time scale, τ. We then introduce the chiral chemical potential, μ_5, conjugated to the value of n_5 at equilibrium. In our study, we compute the value of μ_5 self-consistently by coupling the gap equation to the number equation. As a consequence, μ_5 depends on temperature as well as on external fields, and on the relaxation time which brings information about the microscopic processes that lead to chiral density relaxation.

In the second part of this talk, we focus on the role of chirality production on T_c. As mentioned above, the $\boldsymbol{E}\cdot\boldsymbol{B}$ term tends to lower the critical temperature; on the other hand, the chiral chemical potential has the effect to increase T_c [22, 23, 28–33]. Therefore, it is interesting to compute the response of T_c to the simultaneous presence of μ_5 and fields to check whether the inverse catalysis scenario obtained at $\mu_5=0$ still persists at $\mu_5\neq 0$. We find that chiral density does not affect drastically the thermodynamics at the phase transition, confirming the inverse catalysis induced by the fields, at least if the average chiral chemical potential in the crossover region turns out to be small with respect to temperature.

2 The model

We are interested to study quark matter in a background made of parallel electric, $\boldsymbol{E}$, and magnetic, $\boldsymbol{B}$, fields. We assume the fields are constant in time and homogeneous in space; moreover, we assume they develop along the $z-$direction. For concrete calculations we use a Nambu–Jona–Lasinio (NJL) model [55–58] with a local interaction kernel. The setup of the gap equation has been presented in great detail in [54], therefore, we will skip all the technical details and report here only the few equations we need to specify the interactions used in the calculations. The Euclidean Lagrangian density is given by

$$\mathcal{L}=\bar{\psi}(i\not{D}-m_0)\psi+G\left[(\bar{\psi}\psi)^2+(\bar{\psi}i\gamma_5\boldsymbol{\tau}\psi)^2\right], \tag{1}$$

with ψ being a quark field with Dirac, color, and flavor indices, m_0 is the current quark mass, and $\boldsymbol{\tau}$ denotes a vector of Pauli matrices on flavor space. The interaction with the background fields is embedded in the covariant derivative $\not{D}=(\partial_\mu-iA_\mu\hat{q})\gamma_\mu$, where γ_μ denotes the set of Euclidean Dirac matrices and $\hat{q}$ is the quark electric charge matrix in flavor space. In this work, we use the gauge $A_\mu=(iEz,0,-Bx,0)$.

Introducing the auxiliary field $\sigma=-2G\bar{\psi}\psi$, and, within the mean field approximation, the thermodynamic potential can be written as

$$\Omega=\frac{(M_q-m_0)^2}{4G}-\frac{1}{\beta V}\mathrm{Tr}\log\beta(i\not{D}-M_q), \tag{2}$$

where the constituent quark mass is $M_q=m_0-2G\langle\bar{\psi}\psi\rangle$, $\beta=1/T$, and βV corresponds to the Euclidean quantization volume. The constituent quark mass differs from m_0 because of spontaneous chiral symmetry breaking, the latter being related to a nonvanishing chiral condensate, $\langle\bar{\psi}\psi\rangle\neq 0$. Even if it would be more appropriate to discuss chiral symmetry restoration via the quark condensate, because it has its counterpart in QCD, we will refer to M_q for simplicity, keeping in mind that whenever we discuss about the chiral phase transition in terms of M_q, the decrease of the latter is related to the decreasing of magnitude of the chiral condensate.

The main technical task is to compute M_q at finite temperature and in presence of the external fields: This is achieved by requiring the physical value of M_q minimizes the thermodynamic potential, and this in turn implies that M_q satisfies the gap equation, $\partial\Omega/\partial M_q=0$, namely

$$\frac{M_q-m_0}{2G}-\frac{1}{\beta V}\mathrm{Tr}\mathcal{S}(x,x')=0, \tag{3}$$

where $\mathcal{S}(x,x')$ corresponds to the full fermion propagator in the electric and magnetic field background. The computation of the propagator has been already given in detail in [54], namely

$$\begin{aligned}\frac{M_q-m_0}{2G}=&\,M_q\frac{N_c}{4\pi^2}\sum_f\int_0^\infty\frac{ds}{s^2}e^{-M_q^2 s}\mathcal{F}(s)\\&+M_q\frac{N_cN_f}{4\pi^2}\int_{1/\Lambda^2}^\infty\frac{ds}{s^2}e^{-M_q^2 s},\end{aligned} \tag{4}$$

where we have defined

$$\mathcal{F}(s) = \theta_3\left(\frac{\pi}{2}, e^{-|\mathcal{A}|}\right)\frac{q_f eBs}{\tanh(q_f eBs)}\frac{q_f eEs}{\tan(q_f eEs)} - 1 \tag{5}$$

with $\theta_3(x,z)$ being the third elliptic theta function, and

$$\mathcal{A}(s) = \frac{q_f eE}{4T^2 \tan(q_f eEs)}. \tag{6}$$

In Eq. (4), we have added and subtracted the zero field contribution on the right-hand side which is the only one to diverge, and we have regularized it by cutting the integration at $s = 1/\Lambda^2$; on the other hand, we have not added a cutoff on the field dependent part. In calculations, we use the standard parameter set for a proper time regularization [57], namely $\Lambda = 1086$ MeV and $G = 3.78/\Lambda^2$.

The presence of the $1/\tan(q_f eEs)$ in Eq. (5) implies the existence of an infinite set of poles on the integration in s in Eq. (4). Following the treatment by Schwinger [59], these poles are shifted from the real axis to the complex plane by adding a small imaginary part which allows to perform the $s-$integration in principal value; this leads to an imaginary part of the free energy, which is a sign of the vacuum instability induced by the static electric field [59, 60] and leads to particle pair creation. We will consider the effect of this vacuum instability in Sect. 3.4 because it can be directly connected to chiral density production in case of parallel $\boldsymbol{E}$ and $\boldsymbol{B}$.

3 Results and the suggested phase diagram

3.1 Zero temperature

The main goal of our study is to compute the combined effect of the electric and magnetic background on the chiral phase transition. In Fig. 1, we plot M_q as a function of eB for several choices of E, starting from $E = 0$ up to $E = B$; for comparison, we also show the case $B = 0$ (green dashed line). In the case $E = 0$, the system experiences a direct magnetic catalysis (DMC), namely M_q increases with B. On the other hand, for $E = 0.5B$, we find a sign of competition among DMC induced by B and inverse catalysis (IC) induced by E (and also by $\boldsymbol{E}\cdot\boldsymbol{B} \neq 0$ as we specify later), which manifests in a nonmonotonic behavior of M_q versus eB. The IC becomes more evident by increasing the value of E / B. The inverse catalysis effect induced by the electric field and the second electromagnetic invariant, $\boldsymbol{E}\cdot\boldsymbol{B}$, is in agreement with previous studies at zero temperature [44–48].

The behavior of M_q for small values of the fields can be understood quantitatively at $T = 0$ and $m_0 = 0$; in fact, in this case, we can find an analytical solution for the gap

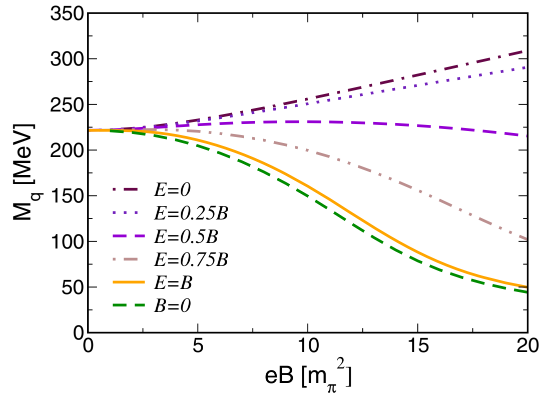

Fig. 1 Dynamical quark mass versus magnetic field strength at zero temperature, for several values of the background electric field. Maroon *dot-dashed line* corresponds to the case of a pure magnetic field, *indigo dotted line* to $E = 0.25B$, *dashed magenta line* to $E = 0.5B$, *dot–dot-dashed brown line* to $E = 0.75B$ and finally *orange line* to $E = B$. For comparison, we have also shown data for $B = 0$; in this case on $x-$axis, we show eE in units of m_π^2. Adapted from Ref. [36]

equation by writing $M_q = M_0 + \delta m$, where M_0 corresponds to the solution of the gap equation for in the zero field case. We find

$$\delta m = \frac{1}{2N_f|\mathcal{E}_i(-M_0^2/\Lambda^2)|}(\Upsilon_1 + \Upsilon_2), \tag{7}$$

where

$$\Upsilon_1 = \frac{q_u^2 + q_d^2}{3M_0^3}\mathcal{I}_1, \tag{8}$$

$$\Upsilon_2 = -\frac{q_u^4 + q_d^4}{45M_0^7}(\mathcal{I}_1^2 + 7\mathcal{I}_2^2), \tag{9}$$

with $\mathcal{I}_1 \equiv (eB)^2 - (eE)^2$, $\mathcal{I}_2 \equiv (eE)(eB)$; moreover, $\mathcal{E}_i$ denotes the exponential integral function, $\mathcal{E}_i(x) = -\int_{-x}^{\infty} dse^{-s}/s$. From Eq. (7), we notice that for $B = 0$, $\delta m \propto -E^2/M_0^3$ at the lowest order; the curvature of δm versus eE does not change as long as $eE > eB$. For $E = B$ one has to take into account the contribution $O(E^2B^2)$ which still shows $\delta m \propto -E^2B^2/M_0^7$ leading to a decreasing M_q. Finally, for $eB > eE$ the catalysis sets in, at least for small values of the fields, eventually leading to $\delta m \propto B^2/M_0^3$ for $E = 0$.

3.2 Finite temperature

The situation depicted in the previous subsection is qualitatively unchanged at finite temperature. In Fig. 2, we plot M_q versus T for several values of E and B: Thin lines correspond to $B = 0$, while with thick lines we denote the results for $E = B$. The blue solid line corresponds to

$eE = m_\pi^2$, orange dotted line to $eE = 8m_\pi^2$, and green dashed line to $eE = 15m_\pi^2$. Increasing the electric field strength results in a lowering of the critical temperature, and the effect of $B \neq 0$ is just to increase a bit the quark mass and shifts the critical temperature toward slightly higher values. The results collected in Fig. 2 show that, even when $B = E$, the effect of the fields on the critical temperature does not cancel and the electric field gives the more important contribution, leading to an inverse catalysis. In fact, one would need a larger value of B to observe an increase of the critical temperature.

3.3 Phase diagram

Using the results discussed in the previous subsections, we are able to suggest a phase diagram in the temperature–electric field strength plane. Firstly we notice that in the case $m_0 \neq 0$, there is no a chiral phase transition, but a smooth crossover, see data in Fig. 2; therefore, we have to chose a criterion to define a pseudo-critical temperature, T_c: In our work, we identify T_c with the temperature at which the maximum of $|dM_q/dT|$ occurs (in the case $m_0 = 0$ T_c is uniquely defined by the temperature at which the condensate is zero). In Fig. 3, we plot T_c versus eE (measured in units of m_π^2) for several values of the external magnetic field: Black squares correspond to $B = 0$, red diamonds to $eB = 5m_\pi^2$ and green triangles to $eB = 10m_\pi^2$. This figure summarizes one of our main results, namely that the electric field leads to a lowering of the critical temperature for chiral symmetry restoration, and the presence of the parallel magnetic field does not change this result unless $B \gg E$.

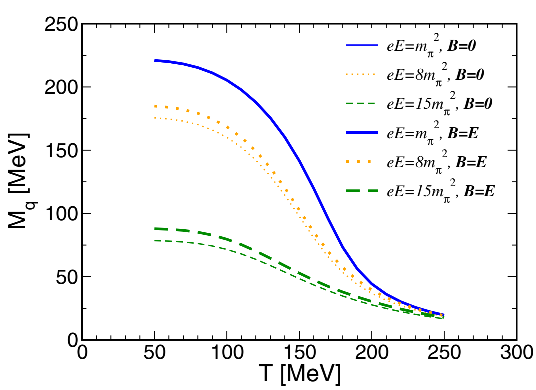

Fig. 2 Dynamical quark mass versus temperature for several values of E and B. *Thin lines* correspond to $B = 0$, while *thick lines* denote the results for $E = B$. The *blue solid line* corresponds to $eE = m_\pi^2$, *orange dotted line* to $eE = 8m_\pi^2$, and *green dashed line* to $eE = 15m_\pi^2$. Color convention for *thick lines* follows that we have used for *thin lines*. Adapted from Ref. [36]

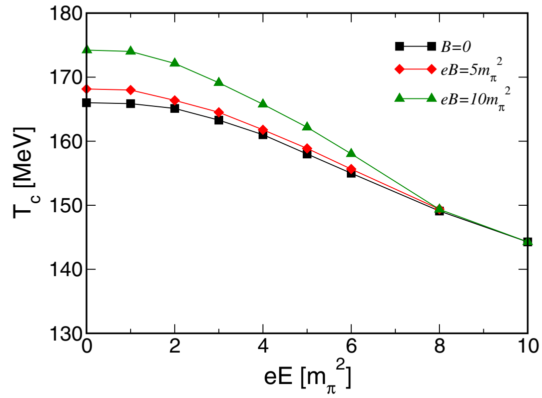

Fig. 3 Critical temperature for chiral symmetry restoration versus electric field strength, measured in units of m_π^2, for several values of the external magnetic field. Adapted from Ref. [36]

3.4 Chiral density effects on the critical temperature

The electric-–magnetic background considered in our study is unstable because of the Schwinger pair production [59, 60]. Once we define the chiral density, $n_5 = n_R - n_L$ where $n_{L/R}$ correspond to left/right-handed particle numbers respectively, quantum anomaly, that is related to the Schwinger effect in this particular case, leads to a dynamical production of n_5 [61]

$$\frac{dn_5}{dt} = \frac{q_f^2(eE)(eB)}{2\pi^2} e^{-\frac{\pi M^2}{|q_f eE|}}. \tag{10}$$

If evolution of n_5 was given only by the above equation, then treating the fields as external, quantum anomaly would lead to an eternal production of n_5, and the system would never be able to reach thermodynamical equilibrium. However, Eq. (10) is just half of the story: As a matter of fact in the thermal bath, there are chirality changing processes which occur on a time scale, τ, that we call the relaxation time of chiral density. The presence of $\tau > 0$ leads to equilibration of n_5. In order to take into account of these processes, we add a relaxation term on the right-hand side of the above equation,

$$\frac{dn_5}{dt} = \frac{q_f^2(eE)(eB)}{2\pi^2} e^{-\frac{\pi M^2}{|q_f eE|}} - \frac{n_5}{\tau}. \tag{11}$$

For $t \gg \tau$ the solution of Eq. (11) relaxes to the equilibrium value

$$n_5^{\rm eq} = \frac{q_f^2(eE)(eB)}{2\pi^2} e^{-\frac{\pi M^2}{|q_f eE|}} \tau; \tag{12}$$

the message encoded in the above equation is that the external fields eventually lead to the production of a medium made of a chiral density, analogously to the medium usually studied in nuclear and particle physics where one considers nuclear and/or quark matter for a finite value of the baryon and/or isospin density.

In Ref. [37], the relaxation time has been computed at the chiral crossover, assuming that the relevant microscopic processes to relax chiral density are quark–quark scattering with the exchange of collective excitations with the quantum numbers of pions as well as $\sigma-$meson. The computation of the relevant collision integrals gives the result for τ in between 0.1 and 2 fm/c around the crossover, with τ decreasing with temperature due to the opening of the phase space. For simplicity in this talk, we summarize results obtained with $\tau = 1$ fm/c in the whole temperature range, neglecting the temperature dependence of τ that eventually would lead to smaller values of n_5.

Equation (12) shows that on a time scale larger than the relaxation time an equilibrium value of n_5, that we name n_5^{eq}, is produced. The existence of n_5^{eq} means it is possible to introduce a chemical potential for the chiral charge, the chiral chemical potential μ_5, conjugated to n_5^{eq}. A self-consistent computation of μ_5, given the value of n_5^{eq} in Eq. (12), requires a canonical ensemble calculation in which the gap equation for M_q is solved self-consistently with the number equation, namely

$$n_5^{\mathrm{eq}} = -\frac{\partial \Omega}{\partial \mu_5}, \tag{13}$$

with μ_5 introduced in the quark propagator with $\boldsymbol{E} \parallel \boldsymbol{B}$. This full calculation is well beyond the purpose of the present study and is left to a future work: Here, we limit ourselves to report results obtained in the limit of small μ_5 as well as small fields. See Ref. [36] for more details.

Taking into account of the equilibrium value of the chiral density is important because it is known that μ_5 leads to an increase of T_{c}, thus working in the opposite direction with respect to the fields in the determination of the critical line. Since μ_5 is produced by the fields themselves, in order to give a firm answer about the net effect of the fields on the phase diagram, we have to consider the backreaction of μ_5 on T_{c}.

In the upper panel of Fig. 4, we plot M_q versus temperature for the case $eE = eB = 8m_\pi^2$ and $n_5 = 0$ (green dots), and we compare it to the case in which n_5 is given by its equilibrium value Eq. (12) (orange dashed line). For matter of comparison, we also show by an indigo solid line the data corresponding to $E = B = 0$. For completeness, in the middle panel of Fig. 4, we plot the equilibrium value of n_5 computed by Eq. (12) as a function of temperature for u quarks (solid indigo line) and d quarks (green dashed line); the orange dot-dashed line corresponds to the average value. The value of n_5 depends on the quark flavor because electric charge is different, see Eq. (12). Finally, in the lower panel of Fig. 4, we show the value of μ_5

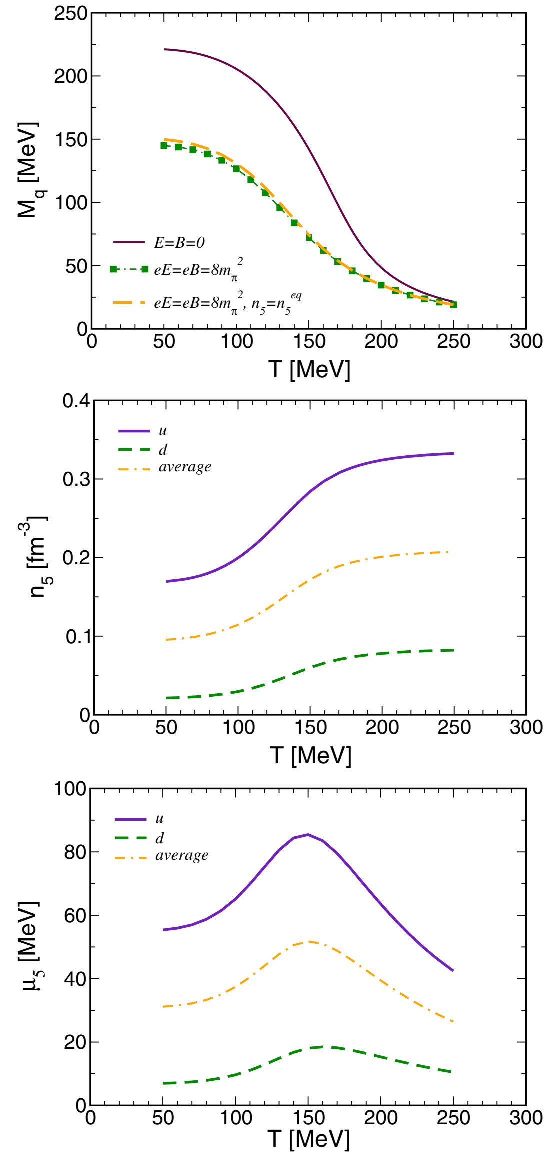

Fig. 4 *Upper panel* M_q versus temperature for the case $eE = eB = 8m_\pi^2$ and $n_5 = 0$ (*green dots*), same values of E and B but with n_5 given by its equilibrium value Eq. (12) (*orange dashed line*). For comparison, we plot by *indigo solid line* the data corresponding to $E = B = 0$. *Middle panel* equilibrium value of n_5 computed by Eq. (12) as a function of temperature for u quarks (*solid indigo line*) and d quarks (*green dashed line*); *orange dot-dashed line* corresponds to the average value. *Lower panel* equilibrium value of μ_5 corresponding to n_5 shown in the *middle panel*, computed by the number equation Eq. (13)

corresponding to n_5 computed by the number equation Eq. (13). We notice that the chiral chemical potential at equilibrium enhances chiral symmetry breaking, in agreement with expectations: Indeed M_q is pushed toward larger values in comparison with the case $\mu_5 = 0$. Compare dots and the dashed line in the upper panel of Fig. 4. When we compute the derivative of M_q with respect to temperature, we also find that T_c is slightly increased by μ_5. However, the net increase of T_c, due to μ_5, is very small in comparison with the lowering of T_c induced by the fields. As a consequence, the equilibrated chiral density does not affect drastically the thermodynamics and the phase diagram.

4 Conclusion

In this talk, we have summarized our results about spontaneous chiral symmetry breaking for quark matter in the background of static, homogeneous and parallel electric field, $\boldsymbol{E}$, and magnetic field, $\boldsymbol{B}$. We have used a Nambu–Jona–Lasinio model to compute the relevant quantities to describe chiral symmetry breaking at finite temperature. We have firstly computed the response of the chiral condensate to the external fields, both at zero and at nonzero temperature. One of the main results is that the critical temperature for chiral symmetry restoration, T_c, is lowered by the simultaneous presence of $E \parallel B$.

We have then considered the effect of equilibration of chiral density, n_5, produced dynamically by axial anomaly on the critical temperature. The equilibration of n_5 happens as a consequence of chirality flipping processes in the thermal bath; we have introduced the relaxation time for chirality, namely τ giving the time scale necessary for the equilibration of n_5. We have focused here on a constant value of $\tau = 1$ fm/c in line with the results of [37]. Because this dynamical system reaches a thermodynamical equilibrium state for $t \gg \tau$, with a specified value of $n_5 = n_5^{\mathrm{eq}}$ depending on the actual values of the field and of the temperature, it is possible to introduce the chiral chemical potential, μ_5, conjugated to n_5^{eq} at equilibrium. The value of μ_5 has been computed by coupling the gap equation to the number equation, solving both within a small μ_5 approximation.

The chiral chemical potential acts as a catalyzer of chiral symmetry breaking; therefore, in principle the background of n_5 can spoil the inverse catalysis induced by $\cdot B$. We have found, however, that the equilibrated chiral density does not change drastically the thermodynamics as long as μ_5 at equilibrium is not too large; that is, the inverse catalysis effect induced by the background fields is eventually not spoiled by the presence of the chiral medium. This can be understood because the increase of T_c, due to μ_5, is much smaller than the lowering induced by the fields. This conclusion might be no longer valid in the case of large μ_5, that probably would be produced by large fields. To study quantitatively the general case, it is necessary to solve simultaneously the number and gap equations without using a small μ_5 approximation that will be the subject of our near future work.

Acknowledgments M. Ruggieri would like to acknowledge fruitful discussions with M. Chernodub and M. Frasca.

References

1. S.L. Adler, Axial vector vertex in spinor electrodynamics. Phys. Rev. **177**, 2426 (1969). doi:10.1103/PhysRev.177.2426
2. J.S. Bell, R. Jackiw, A PCAC puzzle: $\pi^0 \to \gamma\gamma$ in the sigma model. Nuovo Cim. A **60**, 47 (1969). doi:10.1007/BF02823296
3. G. D. Moore, Do we understand the sphaleron rate? arXiv:hep-ph/0009161
4. G.D. Moore, M. Tassler, The sphaleron rate in SU(N) gauge theory. JHEP **1102**, 105 (2011). doi:10.1007/JHEP02
5. D.E. Kharzeev, L.D. McLerran, H.J. Warringa, The effects of topological charge change in heavy ion collisions: 'Event by event P and CP violation'. Nucl. Phys. A **803**, 227 (2008). doi:10.1016/j.nuclphysa.2008.02.298
6. K. Fukushima, D.E. Kharzeev, H.J. Warringa, The chiral magnetic effect. Phys. Rev. D **78**, 074033 (2008). doi:10.1103/PhysRevD.78.074033
7. D.T. Son, P. Surowka, Hydrodynamics with triangle anomalies. Phys. Rev. Lett. **103**, 191601 (2009). doi:10.1103/PhysRevLett.103.191601
8. N. Banerjee, J. Bhattacharya, S. Bhattacharyya, S. Dutta, R. Loganayagam, P. Surowka, Hydrodynamics from charged black branes. JHEP **1101**, 094 (2011). doi:10.1007/JHEP01
9. K. Landsteiner, E. Megias, F. Pena-Benitez, Gravitational anomaly and transport. Phys. Rev. Lett. **107**, 021601 (2011). doi:10.1103/PhysRevLett.107.021601
10. D.T. Son, A.R. Zhitnitsky, Quantum anomalies in dense matter. Phys. Rev. D **70**, 074018 (2004). doi:10.1103/PhysRevD.70.074018
11. M.A. Metlitski, A.R. Zhitnitsky, Anomalous axion interactions and topological currents in dense matter. Phys. Rev. D **72**, 045011 (2005). doi:10.1103/PhysRevD.72.045011
12. D.E. Kharzeev, H.U. Yee, Chiral magnetic wave. Phys. Rev. D **83**, 085007 (2011). doi:10.1103/PhysRevD.83.085007
13. M.N. Chernodub, Chiral heat wave and mixing of magnetic, vortical and heat waves in chiral media. JHEP **1601**, 100 (2016). doi:10.1007/JHEP01
14. M.N. Chernodub, M. Zubkov, Intrinsic chiral magnetic effect in Dirac semimetals due to dislocations. arXiv:1508.03114 [cond-mat.mes-hall]
15. M.N. Chernodub, A. Cortijo, A.G. Grushin, K. Landsteiner, M.A.H. Vozmediano, Condensed matter realization of the axial magnetic effect. Phys. Rev. B **89**(8), 081407 (2014). doi:10.1103/PhysRevB.89.081407
16. V. Braguta, M.N. Chernodub, K. Landsteiner, M.I. Polikarpov, M.V. Ulybyshev, Numerical evidence of the axial magnetic effect. Phys. Rev. D **88**, 071501 (2013). doi:10.1103/PhysRevD.88.071501
17. A.V. Sadofyev, M.V. Isachenkov, The chiral magnetic effect in hydrodynamical approach. Phys. Lett. B **697**, 404 (2011). doi:10.1016/j.physletb.2011.02.041
18. A.V. Sadofyev, V.I. Shevchenko, V.I. Zakharov, Notes on chiral hydrodynamics within effective theory approach. Phys. Rev. D **83**, 105025 (2011). doi:10.1103/PhysRevD.83.105025
19. Z.V. Khaidukov, V.P. Kirilin, A.V. Sadofyev, V. I. Zakharov, On magnetostatics of chiral media. arXiv:1307.0138 [hep-th]
20. V.P. Kirilin, A.V. Sadofyev, V.I. Zakharov, Anomaly and long-range forces. doi:10.1142/9789814616850_0014. arXiv:1312.0895 [hep-ph]
21. A. Avdoshkin, V.P. Kirilin, A.V. Sadofyev, V.I. Zakharov, On consistency of hydrodynamic approximation for chiral media. Phys. Lett. B **755**, 1 (2016). doi:10.1016/j.physletb.2016.01.048
22. M. Ruggieri, G.X. Peng, Critical temperature of chiral symmetry restoration for quark matter with a chiral chemical potential. arXiv:1602.03651 [hep-ph]

23. M. Ruggieri, G.X. Peng, Chiral symmetry restoration with a chiral chemical potential: the role of momentum dependent quark self-energy. arXiv:1602.05250 [hep-ph]
24. R. Gatto, M. Ruggieri, Hot quark matter with a chiral chemical potential. Phys. Rev. D **85**, 054013 (2012). doi:10.1103/PhysRevD.85.054013
25. K. Fukushima, M. Ruggieri, R. Gatto, Chiral magnetic effect in the PNJL model. Phys. Rev. D **81**, 114031 (2010). doi:10.1103/PhysRevD.81.114031
26. M.N. Chernodub, A.S. Nedelin, Phase diagram of chirally imbalanced QCD matter. Phys. Rev. D **83**, 105008 (2011). doi:10.1103/PhysRevD.83.105008
27. M. Ruggieri, The critical end point of quantum chromodynamics detected by chirally imbalanced quark matter. Phys. Rev. D **84**, 014011 (2011). doi:10.1103/PhysRevD.84.014011
28. L. Yu, H. Liu, M. Huang, The effect of the chiral chemical potential on the chiral phase transition in the NJL model with different regularization schemes. arXiv:1511.03073 [hep-ph]
29. L. Yu, J. Van Doorsselaere, M. Huang, Inverse magnetic catalysis in the three-flavor NJL model with axial-vector interaction. Phys. Rev. D **91**(7), 074011 (2015). doi:10.1103/PhysRevD.91.074011
30. M. Frasca, Nonlocal Nambu–Jona–Lasinio model and chiral chemical potential. arXiv:1602.04654 [hep-ph]
31. V.V. Braguta, E.-M. Ilgenfritz, A.Y. Kotov, B. Petersson, S.A. Skinderev, Study of QCD phase diagram with non-zero chiral chemical potential. arXiv:1512.05873 [hep-lat]
32. V.V. Braguta, V.A. Goy, E.-M. Ilgenfritz, A.Y. Kotov, A.V. Molochkov, M. Muller-Preussker, B. Petersson, Two-color QCD with non-zero chiral chemical potential. JHEP **1506**, 094 (2015). doi:10.1007/JHEP06
33. V.V. Braguta, A.Y. Kotov, Catalysis of dynamical chiral symmetry breaking by chiral chemical potential. arXiv:1601.04957 [hep-th]
34. M. Hanada, N. Yamamoto, Universality of phase diagrams in QCD and QCD-like theories. PoS LATTICE **2011**, 221 (2011)
35. S.S. Xu, Z.F. Cui, B. Wang, Y.M. Shi, Y.C. Yang, H.S. Zong, Chiral phase transition with a chiral chemical potential in the framework of Dyson-Schwinger equations. Phys. Rev. D **91**(5), 056003 (2015). doi:10.1103/PhysRevD.91.056003
36. M. Ruggieri, G.X. Peng, Quark matter in a parallel electric and magnetic field background: chiral phase transition and equilibration of chiral density. Phys. Rev. D **93**(9), 094021 (2016). doi:10.1103/PhysRevD.93.094021
37. M. Ruggieri, G.X. Peng, M. Chernodub, Chiral relaxation time at the chiral crossover of quantum chromodynamics. arXiv:1606.03287 [hep-ph]
38. R.L.S. Farias, D.C. Duarte, G. Krein, R.O. Ramos, Quark matter with a chiral imbalance in the Nambu–Jona–Lasinio model. arXiv:1604.04518 [hep-ph]
39. Z.F. Cui, I.C. Cloet, Y. Lu, C.D. Roberts, S.M. Schmidt, S.S. Xu, H.S. Zong, Critical endpoint in the presence of a chiral chemical potential. arXiv:1604.08454 [nucl-th]
40. A.A. Andrianov, D. Espriu, X. Planells, An effective QCD Lagrangian in the presence of an axial chemical potential. Eur. Phys. J. C **73**(1), 2294 (2013). doi:10.1140/epjc/s10052-013-2294-0
41. S.S. Afonin, A.A. Andrianov, D. Espriu, The masses of vector mesons in holographic QCD at finite chiral chemical potential. Phys. Lett. B **745**, 52 (2015). doi:10.1016/j.physletb.2015.04.027
42. D. Ebert, T.G. Khunjua, K.G. Klimenko, V.C. Zhukovsky, Competition and duality correspondence between chiral and superconducting channels in (2+1)-dimensional four-fermion models with fermion number and chiral chemical potentials. Phys. Rev. D **93**(10), 105022 (2016). doi:10.1103/PhysRevD.93.105022
43. B. Wang, Y.L. Wang, Z.F. Cui, H.S. Zong, Effect of the chiral chemical potential on the position of the critical endpoint. Phys. Rev. D **91**(3), 034017 (2015). doi:10.1103/PhysRevD.91.034017
44. A.Y. Babansky, E.V. Gorbar, G.V. Shchepanyuk, Chiral symmetry breaking in the Nambu–Jona–Lasinio model in external constant electromagnetic field. Phys. Lett. B **419**, 272 (1998). doi:10.1016/S0370-2693(97)01445-7
45. S.P. Klevansky, R.H. Lemmer, Chiral symmetry restoration in the Nambu–Jona–Lasinio model with a constant electromagnetic field. Phys. Rev. D **39**, 3478 (1989). doi:10.1103/PhysRevD.39.3478
46. H. Suganuma, T. Tatsumi, On the behavior of symmetry and phase transitions in a strong electromagnetic field. Annals Phys. **208**, 470 (1991). doi:10.1016/0003-4916(91)90304-Q
47. K.G. Klimenko, Three-dimensional Gross–Neveu model at nonzero temperature and in an external magnetic field. Z. Phys. C **54**, 323 (1992). doi:10.1007/BF01566663
48. K.G. Klimenko, Three-dimensional Gross–Neveu model at nonzero temperature and in an external magnetic field. Theor. Math. Phys. **90**, 1 (1992) [Teor. Mat. Fiz. **90**, 3 (1992)]. doi:10.1007/BF01018812
49. I.V. Krive, S.A. Naftulin, Dynamical symmetry breaking and phase transitions in a three-dimensional Gross–Neveu model in a strong magnetic field". Phys. Rev. D **46**, 2737 (1992). doi:10.1103/PhysRevD.46.2737
50. V.P. Gusynin, V.A. Miransky, I.A. Shovkovy, Catalysis of dynamical flavor symmetry breaking by a magnetic field in (2+1)-dimensions. Phys. Rev. Lett. **73**, 3499 (1994), Erratum: [Phys. Rev. Lett. **76**, 1005 (1996)]. doi:10.1103/PhysRevLett.73.3499
51. V.P. Gusynin, V.A. Miransky, I.A. Shovkovy, Dimensional reduction and dynamical chiral symmetry breaking by a magnetic field in (3+1)-dimensions. Phys. Lett. B **349**, 477 (1995). doi:10.1016/0370-2693(95)00232-A
52. G. Cao, X.G. Huang, Electromagnetic triangle anomaly and neutral pion condensation in QCD vacuum. Phys. Lett. B **757**, 1 (2016). doi:10.1016/j.physletb.2016.03.066
53. M. D'Elia, M. Mariti, F. Negro, Susceptibility of the QCD vacuum to CP-odd electromagnetic background fields. Phys. Rev. Lett **110**(8), 082002 (2013). doi:10.1103/PhysRevLett.110.082002
54. G. Cao, X.G. Huang, Chiral phase transition and Schwinger mechanism in a pure electric field. Phys. Rev. D **93**(1), 016007 (2016). doi:10.1103/PhysRevD.93.016007
55. Y. Nambu, G. Jona-Lasinio, Dynamical model of elementary particles based on an analogy with superconductivity. 1. Phys. Rev. **122**, 345 (1961). doi:10.1103/PhysRev.122.345
56. Y. Nambu, G. Jona-Lasinio, Dynamical model of elementary particles based on an analogy with superconductivity. II. Phys. Rev. **124**, 246 (1961). doi:10.1103/PhysRev.124.246
57. S.P. Klevansky, The Nambu–Jona–Lasinio model of quantum chromodynamics. Rev. Mod. Phys. **64**, 649 (1992). doi:10.1103/RevModPhys.64.649
58. T. Hatsuda, T. Kunihiro, QCD phenomenology based on a chiral effective Lagrangian. Phys. Rept. **247**, 221 (1994). doi:10.1016/0370-1573
59. J.S. Schwinger, On gauge invariance and vacuum polarization. Phys. Rev. **82**, 664 (1951)
60. W. Heisenberg, H. Euler, Consequences of Dirac's theory of positrons, Z. Phys. 98, 714. See also arXiv:physics/0605038 for an English translation by W. Korolevski, H. Kleinert. (1936). doi:10.1007/BF01343663
61. H.J. Warringa, Dynamics of the chiral magnetic effect in a weak magnetic field. Phys. Rev. D **86**, 085029 (2012). doi:10.1103/PhysRevD.86.085029